

DEPARTMENT OF PHYSICS
RUTHERFORD SCATTERING AND RANGE OF α PARTICLES

A) RUTHERFORD SCATTERING

1) **Introduction**

This is the classic experiment of Geiger and Marsden (Phil. Mag. 24, 605, 1913) which demonstrated the existence of the nucleus at the center of an orbital atom.

The experiment is 'paired' with another experiment, because most of the readings (Part 2B)- especially those at large scattering angles - require long counting times. Hence the student can get on with other work while counting is progressing.

The apparatus is similar to that shown in Fig 4.2 of Appendix A expect that M is replaced by a modern semiconductor detector (Appendix B).

2) **Procedure**

a) **Preliminaries**

- (1) Make sure the scattering chamber is evacuated.
- (2) (**RUTHERFORD (1) ONLY**) Set the discriminator level on the amplifier, obtain counts for the undeflected beam position ($\theta \sim 0^\circ$), as a function of the discriminator reading. Set the latter well above the noise. As the counting rate is high, a 10 second count time will suffice.
(Note:- use the DISCRIMINATOR O/P from the amplifier)
- 3) Establish the centre of the undeflected beam by obtaining counts in the angular range $10^\circ < \theta < -10^\circ$.Again only a short time is required.

b) **Main results and analysis**

Real scattering events are obtained for $\theta \geq 10^\circ$ Since the fractional error of a count, N is $\propto N^{-1/2}$, you should choose as large counting times as practical. For large scattering angles, aim for $N > 50$; for small angles $N \sim 1000$, at least.

Readings near $\theta \cong 90^\circ$ are not feasible, as the scattered α would have to travel through a considerable thickness of foil. However with a long count time, counts for $\theta \geq 120^\circ$ say should be possible.

Analyse your results by plotting $\log(N/t)$ vs. $\log [1/\sin^4(\theta/2)]$
where t = counting time

RUTHERFORD (2) ONLY

* USE THE V/A OUTPUT FROM THE CHARGED COUPLED AMPLIFIER *

B. ENERGY LOSS AND RANGE OF α PARTICLES

The theory of the interaction of fast charged particles with matter is quite complex; a brief introduction is given in Appendix C. However in this experiment we are simply measuring the α -particle's energy as a function of pressure, and extrapolating these results to give us the range at atmospheric pressure.

First, using the connecting rod to the foil holder (bottom of chamber) move the foil out of the beam so that it is replaced by a blank hole.

Starting at pressure $P = 0$, and with the semiconductor detector in the $\theta = 0$ position, obtain the pulse height spectrum on the MCA; note the channel number of the position of the peak. Repeat this for increasing P , until the peak disappears.

Calculate E for each P value by assuming that $E \propto$ channel number and that E at $P = 0$ is the unaltered \propto energy for Cm^{244} (5.8 MeV).

Plot a graph of E vs P ; extrapolate to $E = 0$ and from the intercept obtain the range of the α 's at atmospheric pressure given that the distance between source and detector is 8 cm. Compare with the empirical formula for the range, R , in the air at atmospheric pressure:

$$R/cm = 0.318(E/\text{MeV})^{3/2}$$

APPENDIX A

4.2 Rutherford Scattering

The Thomson model of the atom was essentially ruled out by the results of a set of experiments conducted by Ernest Rutherford and his students H. W. Geiger and E. Marsden. Rutherford was investigating radioactivity and had shown that the radiation from uranium consisted of at least two types, which he labeled α and β . He showed, by an experiment similar to that of J.J. Thomson, that q/m for the α particle was half that of the proton. Suspecting that the α particles were doubly ionized helium. Rutherford and his co-workers let a radioactive substance decay in a previously evacuated chamber; Then by spectroscopy they detected ordinary helium gas in the chamber. Realising that this energetic, massive particle would make an excellent probe for investigating other atoms, Rutherford began a series of experiments for this purpose.

In these experiments, a narrow beam of α particles fell on a zinc sulphide screen, which gave off visible light scintillations when struck (Fig 4-2). The distribution of scintillations on the screen was observed when various thin metal foils were placed between it and the source. Most of the particles were either undeflected, or deflected through very small angles of the order of 1° .

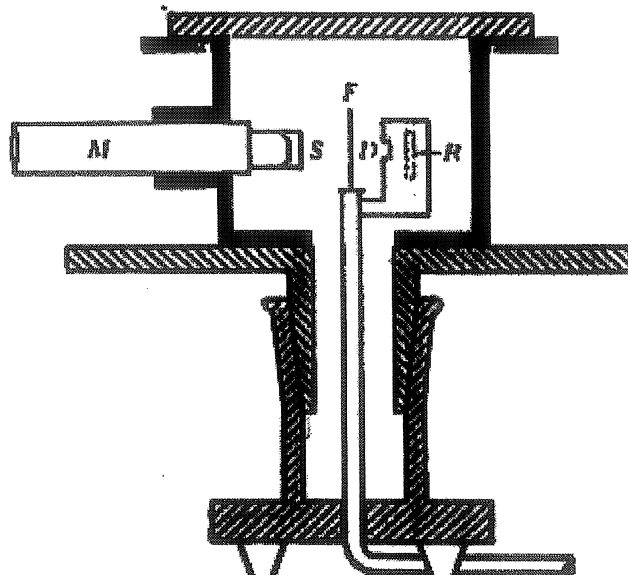


Fig 4.2
Apparatus used by Geiger and Marsden. The α particles from a fixed source R, strike a fixed foil F after passing through a collimating diaphragm D. Scintillations on screen S resulting from scattered particles are observed with a microscope M. The chamber is evacuated and can be rotated about the foil (from H Geiger and E Marsden philosophical Magazine (6)25,507(1913)



Figure 4-3

Head-on (elastic) collision Between an α particle and a light electron. The heavy particle is hardly affected by the collision . Since the relative velocity of seperation after the collisions equals the relative Velocity of approach before The collision, the electrons speed after the collision must be about $2v$

Estimate of deflection due to electrons

Entirely unexpectedly, however, some were deflected through angles as large as 90° . If the atom consisted of a positively charged sphere of radius 10^{-10} m, containing electrons as in the Thomson model, only very small deflection could result from a single encounter between a particle and an atom, even if the α PARTICLE penetrated into the atom. Let us estimate the order of magnitude of the maximum deflection of an α particle in such an encounter. We first consider the collision of an α particle with a single electron. Because the mass of the α particle is about 8000 times that of an electron, the electron can have little effect on the momentum of the α particle. Figure 4.3 shows a head-on collision between a large particle of mass m_α and speed v and a small particle of mass m_e , initially at rest. This is like a collision between a bowling ball and a BB shot. The heavy particle is hardly affected, and continues after the collision with nearly the same speed v . The lighter particle acquires a speed of approximately $2v$ since the relative speed of separation after an elastic collision is the same as the relative speed of approach before the collision. The loss of momentum of the α particle equals the gain in momentum of the electron, which is approximately $2m_e v \approx m_\alpha v / 4000$. We can get an upper-limit estimate on the angle of deflection by taking this maximum momentum change Δp to be perpendicular to the original momentum p of the α particle, as in Figure 4-4. (Of course, Δp could be perpendicular to p only for a glancing collision, in which Δp would be less than $2m_e v$; however, we are Interested only in the order of magnitude of the deflection angle.) Then $\Delta p/p \approx \theta \approx 1/4000 \text{ rad} \approx 0.01^\circ$.

We now consider the possible effect of the positive charge. The electric force on a point charge due to a uniformly charged sphere is shown as a function of r in Figure 4-5. The force is strongest at $r = R$. We can estimate the change in momentum of the α particle, Δp , due to this charge by assuming (that the maximum force acts on it for the time it takes to pass the atom at speed v ; this time is $\Delta t \approx 2R/v$. The force on the particle at a distance R from a positive charge Q is given by Coulomb's law, $F = kq_\alpha Q/R^2$ where q_α is the charge of the α particle and $k = 1/4\pi\epsilon_0 \approx 9 \times 10^9 \text{ N}\cdot\text{m}^2/\text{C}^2$ is the Coulomb constant. The change in momentum is then of the order of

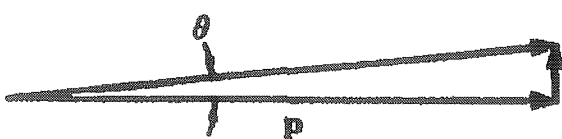


Figure 4-4

The maximum deflection can be estimated by taking the maximum momentum change to be perpendicular to the original momentum.

$$\Delta p \approx \tan \theta = \Delta p / p$$

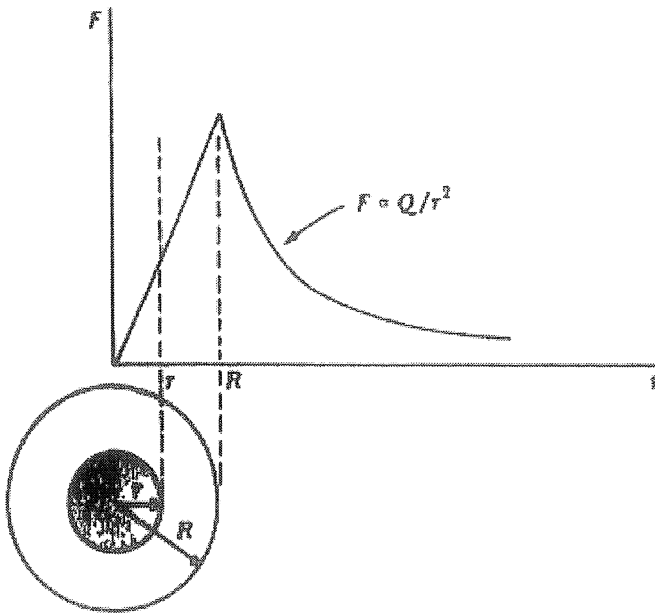


Figure 4.5
 Force on a point charge
 Versus distance r from
 The center of a uniformly charged
 sphere of radius R
 R. Outside the sphere the force is
 proportional to Q/r^2 , where Q is the
 total charge. Inside the sphere, the
 force is proportional to
 $q/r^2 = Qr/R^3$,
 where $q=Q(r/R)^3$ is the charge
 within a sphere of radius r . The
 maximum force occurs at $r=R$

Again taking this change to be at right angles to the original momentum $m_\alpha v$, we get for the maximum deflection angle

$$\tan \theta \approx \frac{\Delta p}{p} = \frac{2kq_\alpha Q}{Rm_\alpha v^2} = \frac{kq_\alpha Q}{R\left(\frac{1}{2}m_\alpha v^2\right)} \quad (4.2)$$

*Estimate of deflection due
 To charged sphere of radius R*

Let us evaluate this expression for a typical case of an α particle of charge $q=2e$. with Energy of 5Mev, incident on a gold atom of $Q=79e$. For this calculation and others, it is Convenient to express the quantity ke^2 , which has dimensions of energy x length, in units of eV-Å or eV-nm .We have

$$ke^2 = (9 \times 10^9 \text{ Nm}^2 / C^2)(1.6 \times 10^{-19} \text{ C})^2$$

$$\times \frac{1 \text{ ev}}{1.6 \times 10^{-19}}$$

$$= 1.44 \times 10^{-9} \text{ eV - nm}$$

$$\text{or } ke^2 = 1.44 \text{ eV - nm} = 14.4 \text{ eV - \AA} \quad (4.3)$$

For our example, Equation 4.2 then gives ,with $R=1 \text{ \AA}$

$$\frac{\Delta p}{p} = \frac{(2)(79)(14.4 \text{ eV - \AA})}{(1 \text{ \AA})(5 \times 10^6 \text{ eV})} = 4.55 \times 10^{-4}$$

Then

$$\tan \theta \approx \theta \approx 4.55 \times 10^{-4} \text{ rad} \approx 0.026^\circ$$

We can see from these crude estimates that a deflection even as small as 1° must be the result Of many collisions, according to the Thomson model of the atom. If this is the case , the number of particles scattered through large angles can be predicted from the statistical theorem of multiple scattering.

For example, a result of this theory (which we shall not derive) is that the fraction scattered through angles greater than some angle θ is $e^{-(\theta/\theta_{RMS})^2}$, where θ_{RMS} is the rms scattering angle. If we take $\theta_{RMS} \approx 1^\circ$, as observed by Geiger and Marsden we obtain for the fraction scattered through 90° or more,

$$e^{-(90/1)^2} = e^{-8100} \approx 10^{-3500}. \text{ The fraction observed was about } \frac{1}{8000}.$$

compared with 10^{-3500}

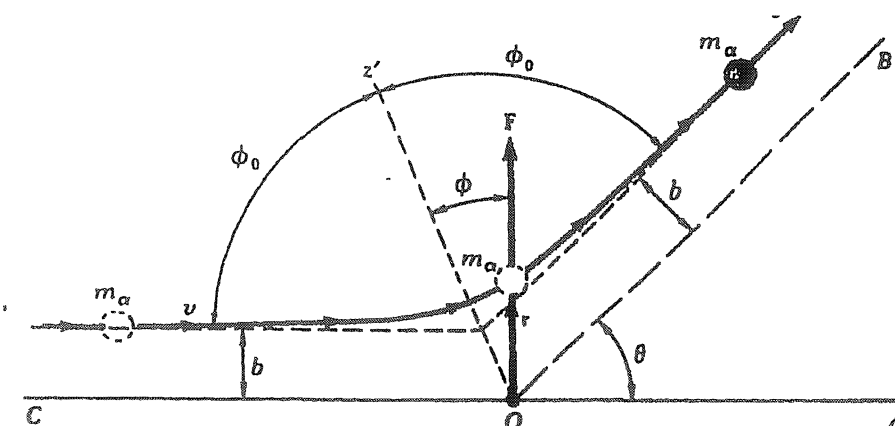
The question is, then, how can one obtain large-angle scattering? The trouble with the Thomson atom is that it is too "soft"—the maximum force experienced by the α particle is too weak to give a large deflection. If the positive charge of the atom is concentrated in a more compact region, however, a much larger force will occur at near impacts. For example, we can take the result of our crude estimate in Equation 4-2 and ask what value of R will give $\Delta p \approx p$. Setting $\tan \theta = 1$ in Equation 4-2 and solving for R , we obtain

$$R = \frac{kq_\alpha Q}{\frac{1}{2} m_\alpha v^2} = \frac{(2)(79)(14.4 \text{ eV} - \text{\AA})}{5 \times 10^6 \text{ eV}} = 4.6 \times 10^{-4} \text{ \AA}$$

Rutherford concluded that such large-angle scattering could result only from a single encounter of the α particle with a massive charge confined to a volume much smaller than that of the whole atom. Assuming this "nucleus" to be a point charge, he calculated the expected angular distribution for the scattered α particles. His predictions as to the dependence of scattering probability on angle, nuclear charge, and kinetic energy were completely verified in a series of experiments carried out in his laboratory by Geiger and Marsden.

We shall not go through Rutherford's derivation in detail, but merely outline the assumptions and conclusions. Figure 4-6 shows the geometry of an α particle being scattered by a nucleus which we take to be a point charge Q at the origin. Initially, the α particle approaches with speed v along a line a distance b from a parallel line COA through the origin. The force on the α particle is

$F = kq_\alpha Q/r^2$, given by Coulomb's law. After scattering, when the α particle is again far from the nucleus, it is moving...



with the same speed v parallel to the line OB , which makes an angle θ with line COA . (Since the potential energy is again zero, the final speed must equal the initial speed by conservation of energy.) The distance b is called the *impact parameter* and the angle θ the scattering angle. The path of the α particle can be shown to be hyperbola and the scattering angle θ can be related to the impact parameter b from the laws of classical mechanics. The result is'

$$b = \frac{kq_\alpha Q}{m_\alpha v^2} \cot \frac{1}{2}\theta \quad (4.4)$$

Impact parameters

*Impact parameters
and Scattering angle*

Figure 4-6 Rutherford scattering geometry. The nucleus is assumed to be a point charge Q at the origin O . At any distance r the α particle experiences a repulsive force $kq_\alpha Q/r^2$. The α particle travels along a hyperbolic path that is initially parallel to line OA a distance b from it and finally parallel to line OB , which makes an angle θ with OA . The scattering angle θ can be related to the impact parameter b by classical mechanics.

Of course, it is not possible to choose or to know the impact parameter for any α particle; but all such particles with impact parameters less than, or equal to, a particular b will be scattered through an angle θ greater than or equal to that given by Equation 4-4 (Figure 4-7). Let the intensity of the incident α particle beam be I_0 particles per second per unit area. The number per second scattered by one nucleus through angles greater than θ equals the number per second that have impact parameters less than $b(0)$. This number is $\pi b^2 I_0$.

The quantity πb^2 , which has the dimensions of an area, is called the *cross section* for scattering through angles greater than θ . The cross section is thus defined to be the number scattered per nucleus divided by the incident intensity. The total number of particles scattered per second is obtained by multiplying $\pi b^2 I_0$ by the number of nuclei in the scattering foil (this assumes the foil to be thin enough to make the chance of overlap negligible). Let n be the number of nuclei per unit volume:

$$n = \frac{\rho(g/cm^3)N_A(atoms/mole)}{M(g/mole)} = \frac{\rho N_A}{M} \frac{atoms}{cm^2}$$

A derivation of this result is given at the end of this section

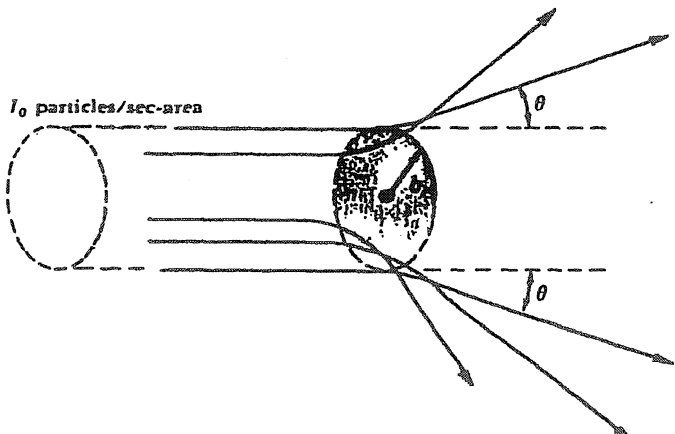


Figure 4-7

Particles with impact parameters less than or equal to b are scattered through angles greater than or equal to θ , related to b by equation 4.4. The area πb^2 is called the cross section for scattering through angles greater than θ

Area a of Beam

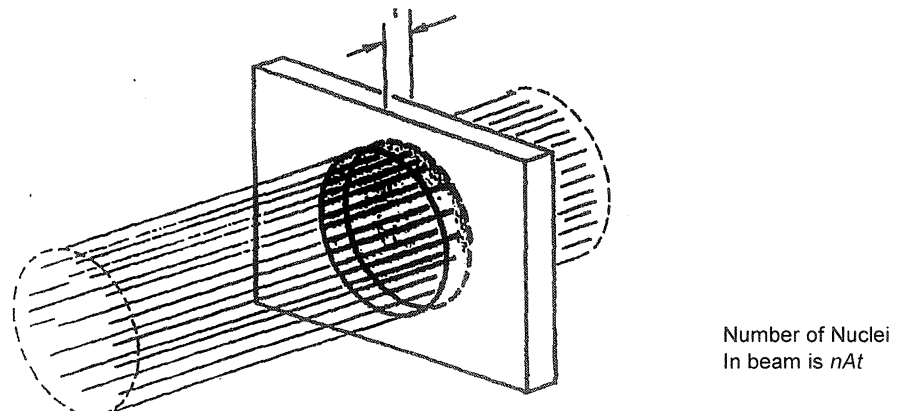


Figure 4-8

The total number of nuclei in the beam is nAt , where n is the number of atoms per unit volume, A is the area of the beam, and t is the thickness of the foil.

For a foil of thickness t the total number of nuclei is nAt , where A is the area of the beam (Figure 4-8). The total number scattered per second through angles greater than θ is thus $\pi b^2 I_0 nt A$.

If we divide this by the number of particles incident per second, $I_0 A$, we get the fraction scattered through angles greater than θ

$$f = \pi b^2 nt \quad (4.6)$$

Let us evaluate this fraction for the gold foil 10^{-4} cm thick, used by Geiger and Marsden, for $\theta = 90^\circ$. Using $\cot(90/2) = 1$ and

taking $\frac{1}{2} m_\alpha v^2 = 5 \text{ Mev}$ for a typical α particle energy, we have,

from Equation 4-4,

$$b = \frac{(2)(79)ke^2}{m_\alpha v^2} = \frac{(2)(79)(14.4eV - \text{\AA})}{(2)(5 \times 10^6 eV)} \approx 2.3 \times 10^{-4} \text{\AA}$$

and from Equation 4-5,

$$n = \frac{(19.3 \text{ g/cm}^3)(6.02 \times 10^{23} \text{ atoms/mole})}{107 \text{ g/mole}} = 5.9 \times 10^{22} \text{ atoms/cm}^3$$

Thus

$$f = \pi(2.3 \times 10^{-12})^2 (5.9 \times 10^{22})(10^{-4}) \approx 10^{-4}$$

This is in good agreement with their observation of about 1 in 8000 in their first trial. Geiger and Marsden did a series of experiments in which they measured:

1. The number of particles per unit area on the screen, scattered through angles between θ and $\theta + d\theta$
2. The variation in the number scattered with foil thickness
3. The variation in the number scattered with the atomic weight of the foil
4. The variation in the number scattered with incident velocity v , which they varied by placing thin absorbers in the incident beam to slow down the α particles

The number scattered by one nucleus at angles between θ and $\theta + d\theta$ is the number incident with impact parameters between b and $b + db$ (Figure 4-9). This number equals the product of the incident intensity I_0 and the area $2\pi b db$ shown in Figure 4-9. We shall omit the algebraic details of the calculation of this number from Equation 4-4. The result can be written

$$I_0 2\pi b db = I_0 2\pi \left(\frac{kZr^2}{m_\alpha v^2} \right)^2 \frac{\sin \theta d\theta}{\sin^4 \frac{1}{2}\theta} \quad (4.7)$$

The area of the screen, from Figure 4.10, is $(2\pi r \sin \theta) (r d\theta)$. The number scattered by one nucleus per unit area on the screen is therefore proportional to

$$\frac{N}{Area} \propto I_0 \left(\frac{kZr^2}{m_\alpha v^2} \right)^2 \frac{1}{\sin^4 \frac{1}{2}\theta} \quad (4.8)$$

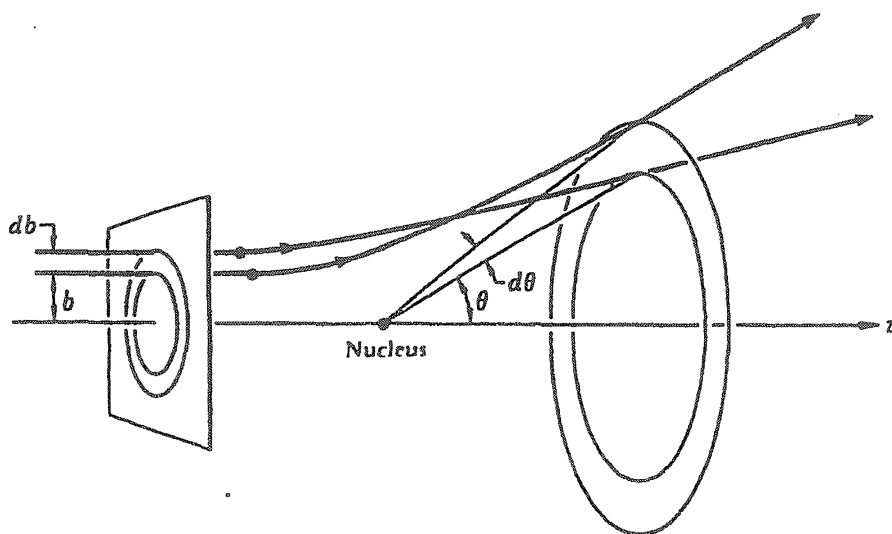


Figure 4-9
The number of particles with impact parameters between b and $b + db$ is proportional to the area $2\pi b db$. These particles are scattered into the range $d\theta$.

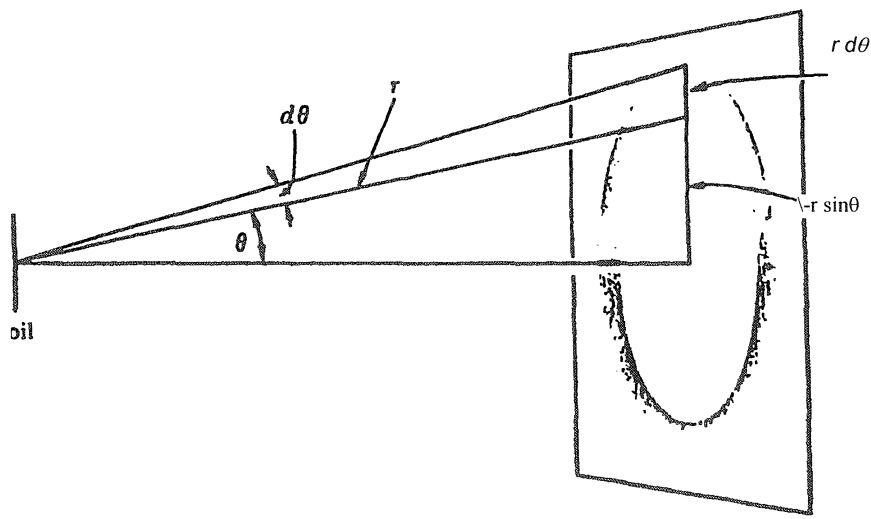


Figure 4-10
Particles scattered into the range $d\theta$, fall on the shaded area on the screen. This area is $(r d\theta)(2r \sin\theta)$

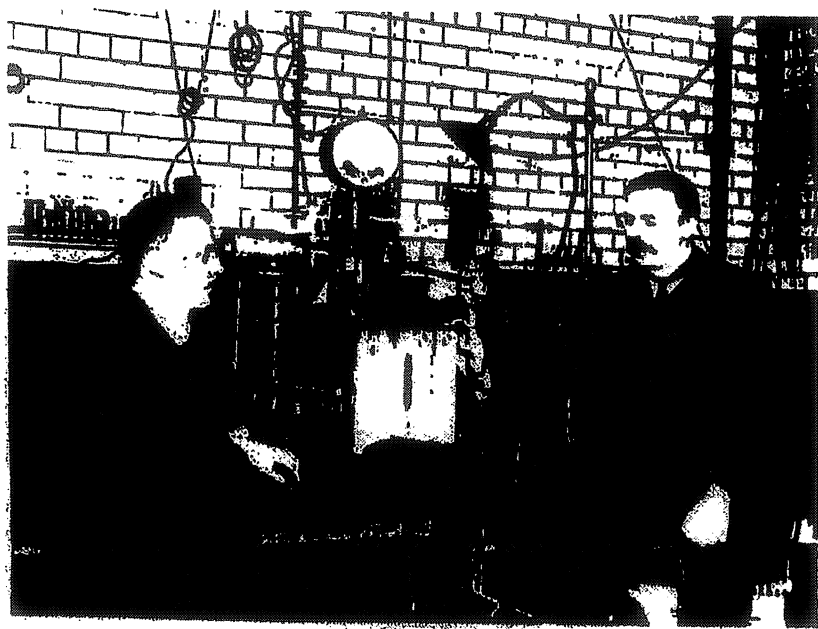
portional to $\sin^{-4}(\theta/2)$, to Z^2 , and to v^{-4} . Since the number of scattering nuclei is proportional to the foil thickness, the number of particles scattered at a given angle should be proportional to the foil thickness if the scattering is due to a single encounter between the α particle and a nucleus.

We quote the summary from the paper "Deflection of α Particles through Large Angles," by Geiger and Marsden, *Philosophical Magazine* (6), 25, 605 (1913).

The experiments described in the foregoing paper were carried out to test a theory of the atom proposed by Prof. Rutherford, the main feature of which is that there exists at the center of the atom an intense, highly concentrated electrical charge. The verification is based on the laws of scattering which were deduced from this theory. The following relations have been verified experimentally:

1. The number of α particles emerging from a scattering foil at an angle θ with the original beam varies as $1/\sin^4(\theta/2)$, when the α particles were counted on a definite area at a constant distance from the foil. This relation has been tested for angles varying from 5° to 150° , and over this range the number of α particles varied from 1 to 250,000 in a good agreement with the theory.
2. The number of α particles scattered in a definite direction is directly proportional to the thickness of the scattering foil for small thicknesses. For large thicknesses the decrease of velocity of the α particles in the foil causes a somewhat more rapid increase in the amount of scattering.
3. The scattering per atom of foils of different materials varies approximately as the square of the atomic weight. This relation was tested for foils of atomic weight from that of carbon to that of gold.

$$N(\theta) \propto \cosec^4\left(\frac{\theta}{2}\right)$$



Hans Geiger (left) and Ernest Rutherford in their Manchester Laboratory.
(Courtesy of University of Manchester.)

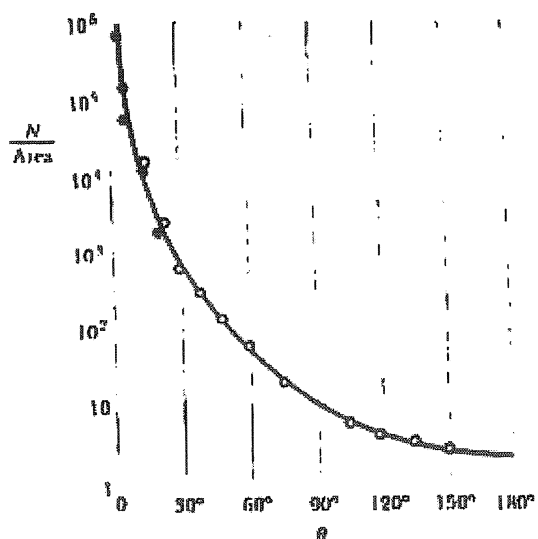


Figure 4-11
The number of scattered α particles as a function of θ . The curve is $\sin^{-1}(1/2)\theta$. The data are from Geiger and Marsden. (From R. D. Evans, *The Atomic Nucleus*, New York: McGraw-Hill Book Company, 1955.)

4. The amount of scattering by a given foil is approximately proportional to the inverse fourth power of the velocity of the incident α particles. This relation was tested over a range of velocities such that the number of scattered particles varied as 1:10.

5. Quantitative experiments show that the fraction of particles of Ra C, which is scattered through an angle of 45° by a gold foil of 1 mm air equivalent (2.1×10^{-6} cm), is 3.7×10^{-7} when scattered particles are counted on a screen of 1-sq mm area placed at a distance of 1 cm from the scattering foil. From this figure and the foregoing results, it can be calculated that the number of elementary charges composing the center of the atom is equal to half the atomic weight.

Figure 4-11 is a plot of their data, showing the angular dependence of the scattering using 7.7-MeV α particles. The excellent agreement of their data with the $\sin^{-1}(1/2)\theta$ prediction of Equation 4-8 indicates that the force law $F = kq_aQ/r^2$ used to derive Equation 4-8 is correct. This does not imply that the nucleus is a mathematical point charge, however; the force law would be the same even if the nucleus were a ball of charge of some radius R_0 , as long as the α particle did not penetrate the ball (Figure 4-12). For a given scattering angle, the distance of closest approach of the α particle to the nucleus can be calculated from the geometry of the collision. For the largest angle, near 180° , the collision is nearly "head on." The corresponding distance of closest approach thus is an experimental upper limit on the size of the target nucleus.

We can calculate the distance of closest approach for a head-on collision r_d by setting the potential energy at this distance equal to the original kinetic energy:

$$\frac{kq_aQ}{r_d} = \frac{1}{2}m_a v^2$$

or

$$r_d = \frac{kq_aQ}{\frac{1}{2}m_a v^2} \quad 4-9$$

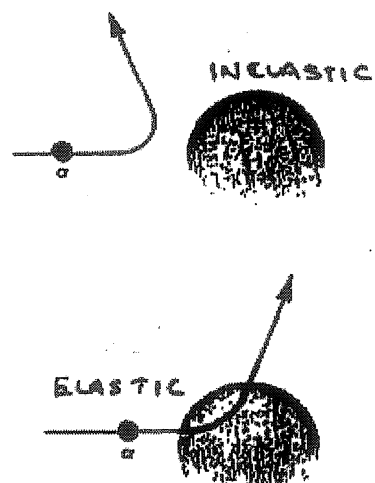


Figure 4-12
If the α particle does not penetrate the nuclear charge, the nucleus can be considered a point charge. If the particle has enough energy to penetrate the nucleus, as in the figure on the bottom, the Rutherford scattering law does not hold.

For the case of 7.7-MeV α particles, the distance of closest approach for a head-on collision is

$$r_0 = \frac{(2)(79)(14.4 \text{ eV}\cdot\text{\AA})}{7.7 \times 10^6 \text{ eV}} \approx 3 \times 10^{-14} \text{ \AA} = 3 \times 10^{-14} \text{ m}$$

For other collisions, the distance of closest approach is somewhat greater than this, but for those scattered at large angles it is of the same order of magnitude. The excellent agreement of the data of Geiger and Marsden at large angles with the prediction of Equation 4-8 thus indicates that the radius of the gold nucleus is less than about 3×10^{-14} m. If higher-energy particles could be used, the distance of closest approach would be smaller, and as the energy of the α particles increased, we might expect that eventually the particles would penetrate the nucleus. Since, for this case, the force law is no longer $F = kq_1Q/r^2$, the data would not agree with the point-nucleus calculation. Rutherford did not have higher-energy α particles available, but he could reduce the distance of closest approach by using targets of lower atomic numbers. For the case of aluminum with $Z = 13$, the most energetic α particles scattered at large angles did not follow the predictions of Equation 4-8. From these data, Rutherford estimated the radius of the aluminum nucleus to be about 10^{-14} m.

A unit of length convenient for describing nuclear sizes is the fermi, or femtometer (fm), defined by 1 fm = 10^{-15} m. As we shall see in Chapter 11, the nuclear radius varies from about 1 to 10 fm from the lightest to the heaviest atoms.

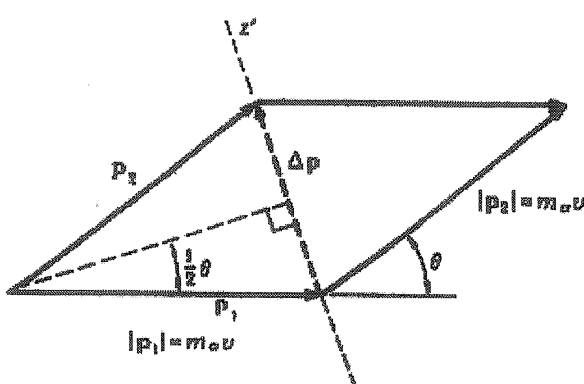
Optimal

Derivation of Equation 4-4

We can derive the relation between the impact parameter b and the scattering angle θ as given by Equation 4-4 without going into the details of finding the path followed by the α particle.

Let \mathbf{p}_1 and \mathbf{p}_2 be the initial and final momentum vectors of the α particle. From Figure 4-13 it is evident that the total change in momentum $\Delta \mathbf{p} = \mathbf{p}_2 - \mathbf{p}_1$ is along the z' axis of Figure 4-6. The

Figure 4-13
Momentum diagram for Rutherford scattering. The magnitude of the momentum change Δp is related to the scattering angle θ by $\Delta p = 2m_\alpha v \sin \frac{1}{2}\theta$.



magnitude of either P_1 or P_2 is $m_\alpha v$. From the isosceles triangle formed by P_1 , P_2 and ΔP shown in Figure 4.13 we have

$$\frac{\frac{1}{2}\Delta P}{m_\alpha v} = \sin \frac{1}{2}\theta$$

or $\Delta P = 2m_\alpha v \sin \frac{1}{2}\theta$

We now write Newton's law for the α particle: $F = dp/dt$. Or

$$dp = F dt$$

The force F is given by Coulombs law, $F = kq_\alpha Q/r^2$, and is in the radial direction.

Taking components along the Z' direction and integrating to obtain ΔP , we have

$$\Delta P = \int (dp)_{Z'} = \int F \cos \phi dt = \int F \cos \phi \frac{dt}{d\phi} d\phi \quad (4.11)$$

where we have changed the variable of integration from t to the angle ϕ .

We can relate $dt/d\phi$ to the angular momentum of the α particle about the origin.

Since the force is central (i.e., acts along the line joining the α particle and the nucleus at the origin), there is no torque about the origin. and the angular momentum of the α particle is conserved, Initially, the angular momentum has the magnitude $m_\alpha vb$. At a later time, it is $m_\alpha r^2 d\phi/dt$. Conservation of angular momentum thus gives

$$m_\alpha r^2 \frac{d\phi}{dt} = m_\alpha vb$$

or

$$\frac{dt}{d\phi} = \frac{r^2}{vb}$$

Substituting this result and $F = kq_\alpha Q/r^2$ for the force into Equation 4.11 we obtain

$$\Delta P = \int \frac{kq_\alpha Q}{r^2} \cos \phi \frac{r^2}{vb} d\phi = \frac{kq_\alpha Q}{vb} \int \cos \phi d\phi$$

or

$$\Delta P = \frac{kq_\alpha Q}{vb} (\sin \phi_2 - \sin \phi_1)$$

From Figure 4-6 we see that $\phi_1 = -\phi_0$ and, $\phi_2 = +\phi_0$, where $2\phi_0 + \theta = 180^\circ$.

Then $\sin \phi_2 - \sin \phi_1 = 2\sin(90^\circ - \frac{1}{2}\theta) = 2\cos \frac{1}{2}\theta$

Combining Equations 4-10 and 4-12 for ΔP we have

$$\Delta P = 2m_\alpha v \sin \frac{1}{2}\theta = \frac{kq_\alpha Q}{vb} 2 \cos \frac{1}{2}\theta \quad \text{or} \quad b = \frac{kq_\alpha Q}{m_\alpha v^2} \cot \frac{1}{2}\theta$$

Which is equation 4.4

APPENDIX B

From "Fundamentals of Nuclear Physics ", Adam P. Arya

Solid State Detector

The use of some semiconductor (or dielectric) crystals as detectors was demonstrated by P Van Heerden⁽³²⁾ in 1945 and D. Wooldridge, *et al*⁽³³⁾ in 1947. Since then , semiconductors have been used for the detection of charged particles in several ways⁽³⁴⁻³⁸⁾. A germanium P-N junction diode has been used as an alpha-particle detector by K Mckay⁽³⁴⁾ and R Bomal et al⁽³⁸⁾ .Very recently a diffused-junction silicon detector has been developed⁽³⁹⁾ and used successfully for charged particle counting. We shall describe in some detail the workings of such a solid-state detector.

An atom of silicon has four valence electrons and, as a result, it is a poor conductor of electricity at room temperature. The conduction band of silicon lies 1.1ev above the valence band. If an atom of Phosphorous, which has five valence electrons, is introduced into silicon, four electrons are used

up

in bond formation while the fifth electron goes near the conduction band (Fig 3.12a)

The Phosphorous is the donor ,and the silicon, thus containing traces of Phosphorous, becomes N-type silicon. Similarly, If a boron atom , which has three valence electrons , is introduced into silicon, one of the valence electrons of silicon jumps to the boron atom, and lies just above the valance band of silicon, thus creating a " hole " in the valance band of silicon (Fig 3.12b)

The boron is the acceptor, and the silicon, thus containing traces of boron, becomes P- type silicon

N-type and P-type silicon are fused together to form a single crystal calle a P-N junction. A contact potential is established between the two types of materials, the P-type being at a lower potential with respect to N-type.

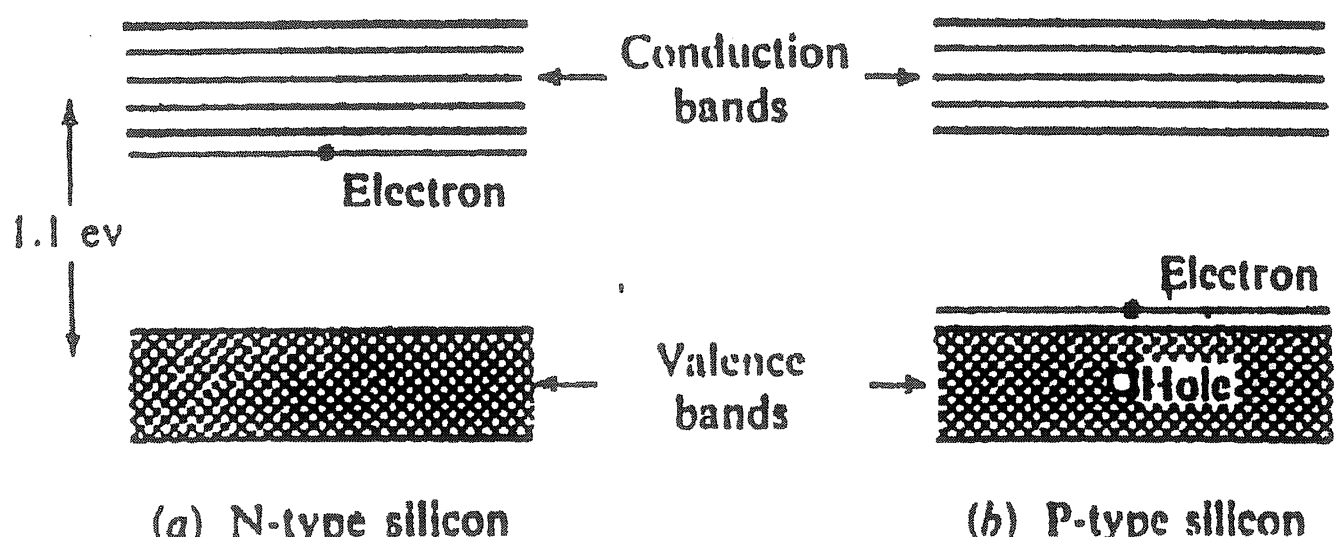


FIG. 3.12 Valence and bound-electron diagram for silicon.

- (a) Silicon containing a trace of phosphorus is called N-type silicon (the donors) and (b) silicon containing a trace of boron is called P-type silicon (the acceptor).

The free electrons of the donor go to the acceptor, thus making the region a nonconductor. This region, the *depletion region*, can be increased still further by the application of an external voltage. The device is shown in Fig. 3.13. The thickness of the depletion region is the sum of the t_n and t_p thicknesses, where

$$t_n = \frac{\epsilon V}{2\pi e N_n} \quad (3.5)$$

$$t_p = \frac{\epsilon V}{2\pi e N_p} \quad (3.6)$$

V is the applied voltage, e the electron charge, c the dielectric constant of silicon, and N_n and N_p are the number of N-type and P-type atoms, respectively, in a unit volume of silicon.

When an ionizing particle enters from the N-type layer and stops in the depletion region, free electrons and holes (positive ions) will be formed. The electrons and the holes move at once towards the N-type (positive) and P-type (negative) layers, respectively. This results in a potential drop across the junction, which is conveyed to the amplifier. The size of the pulse produced is proportional to (the energy of the incident particle) provided the particle loses all its energy in the depletion region. An important feature of such a detector is that the collection time of the electrons and of the holes is very short (less than 10^{-8} second), because the positive ions do not move bodily.

They contribute their share of current by capturing electrons from the neutral atoms, for example, on their right. The neutral atom that has lost an electron to the hole is now a positive ion. Thus, in this process, the hole has moved to the right and the electron to the left.

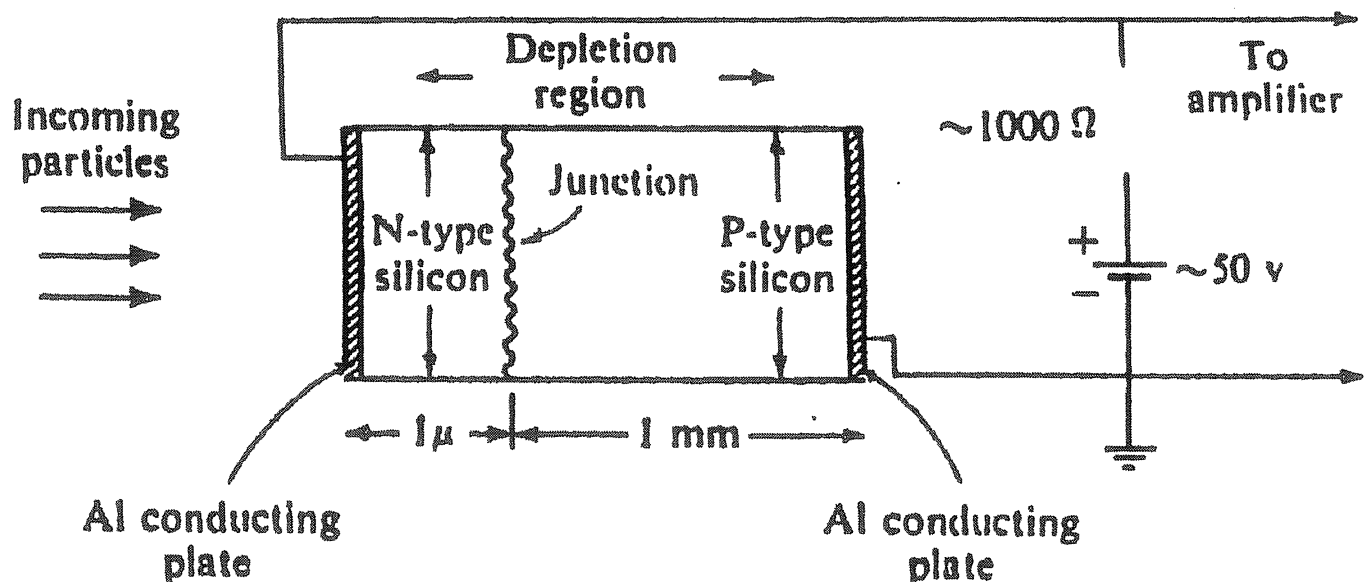


FIG. 3.13 A typical silicon P-N junction detector. The junction is about 1 micron from the surface and the sensitive volume is about 1 mm. (From Friedland, Mayer and Wiggins. Nucleonics 18. 2. 54 (1960).]

This counter has proved to be useful for detecting heavy charged particles such as protons and alpha particles. A typical energy resolution⁽³⁹⁾ for 5.3 Mev alpha particles is found to be 0.6 percent in a 300 ohm-cm detector

with a 6-volt bias. Crystals having depletion depths of the order of 3 to 6 mm have been used for beta and gamma-ray spectroscopy as well. For example, a lithium-drifted germanium crystal, when used at a temperature of 77 K, gives a resolution of \sim 6 Kev for 661 Kev gamma rays of Cs^{137} . For comparison Fig. 3.14 shows a gamma spectrum of Co^{60} obtained by using Li-drifted Ge and the scintillation NaI(Tl) crystals. The excellent resolution of the solid-state crystal (Li-drifted Ge) is quite obvious.

There are several advantages to using semiconductor detectors. (1) They are small in size. (2) They have a fast response. (3) They eliminate the need for a high-voltage supply. (4) They can be designed to give a high-energy resolution response proportional to the incident energy. One big disadvantage of these detectors is that they have a very low efficiency of detection.

APPENDIX C

(From "introductory Nuclear physics" , K.S. Krane

INTERACTIONS OF RADIATION WITH MATTER

Heavy Charged Particles

Although Coulomb scattering of charged particles by nuclei (called Rutherford scattering) is an important process in nuclear physics, it has very little influence on the loss in energy of a charged particle as it travels through the detector material. Because the nuclei of the detector material occupy only about 10^{-15} of the volume of their atoms, it is (crudely) 10^{15} times more probable for the particle to collide with an electron than with a nucleus. The dominant mechanism for energy loss by charged particles is therefore Coulomb scattering by the atomic electrons of the detector.

Conservation of energy and momentum in a head-on elastic collision between a heavy particle of mass M and an electron of mass m (which we assume to be at rest for the sake of this simplified discussion) gives for the loss in kinetic energy of the particle

$$\Delta T = T \left(\frac{4m}{M} \right) \quad (7.1)$$

For a 5Mev α (typical of those emitted in radioactive decay). This amounts to 2.7 Kev

Four conclusions follow immediately:

1. It takes many thousands of such events before the particle loses all its energy (A head-on collision gives the *maximum* energy transfer to the electron: in most collisions, the energy loss of the particle will be much smaller.)
2. In a glancing collision between an electron and a heavy particle, the heavy particle is deflected by a negligible angle, and so the particle follows very nearly a straight-line path.
- 3) Because the Coulomb force has infinite range, the particle interacts simultaneously with many electrons and thus loses energy gradually but continuously along its path. After traveling a certain distance, it has lost all of its energy; this distance is called the *range* of the particle. The range is determined by the type of particle, type of material, and energy of the particle.

Figure 7.1 shows cloud-chamber tracks of α particles; there is a rather well-defined distance beyond which there are no particles. Usually we work with the mean range, defined so that one-half the particles have longer ranges and one-half shorter; the variation about the mean is very small, at most a few percent, so the mean range is a useful and precisely defined quantity.

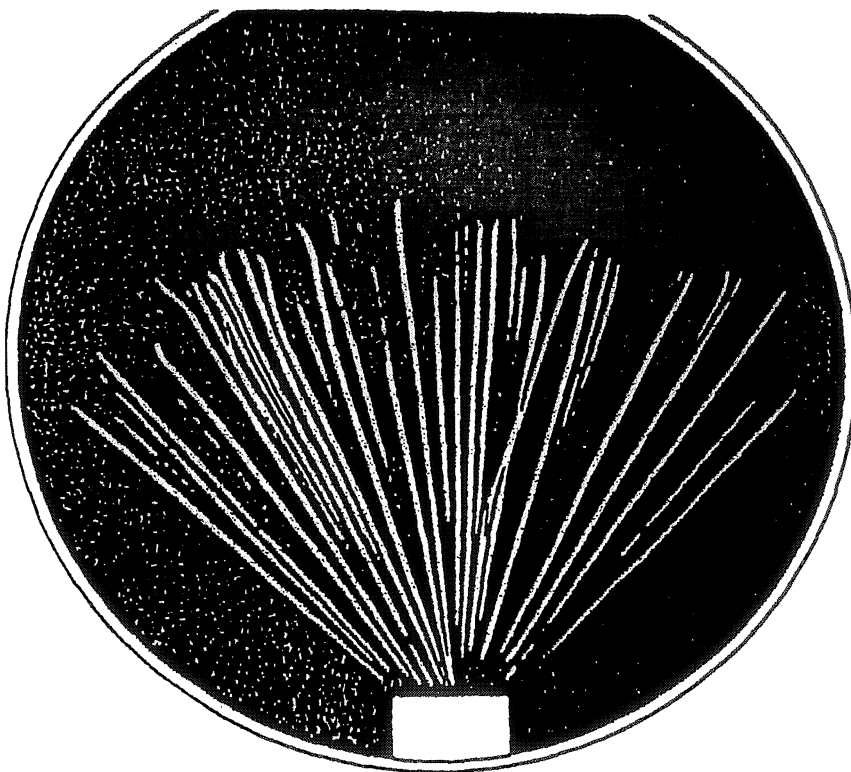


Figure 7.1 Cloud chamber tracks of α particles from the decay of ^{210}Po .

The energy needed ionize an atom (i.e., to remove an electron) is of the order of 10 eV; thus many collisions will transfer enough energy to an electron to ionize the atom. (If the electron is not given enough energy to produce an ion, the atom is placed into an excited state, which quickly de-exites back to the ground state.) Furthermore, electrons given energies in the keV region (which are known as *delta rays*) can themselves produce ions by collisions, resulting in even more *secondary* electrons. To determine the energy lost by the particle, we must include the primary and secondary electrons as well as the atomic excitations,

Figure 7.2 show's the relationship between range and energy for air and for some other commonly encountered materials. For materials that are not shown, an estimate of the range can be made using a semiempirical relationship known as the Bragg-Kleeman rule.

$$\frac{R_1}{R_0} \cong \frac{\rho_0 \sqrt{A_1}}{\rho_1 \sqrt{A_0}} \quad (7.2)$$

Where R is the range, ρ the density and A the atomic weight. The subscripts 0 and 1 refer for instance To the known and unknown ranges and materials respectively.

The theoretical relationship between range and energy can be obtained from a quantum mechanical calculation of the collision process, which was first done in 1930 by Hans Bethe The calculation gives the magnitude of the energy loss per unit length (sometimes called the *stopping power*):

$$\frac{dE}{dx} = \left(\frac{e^2}{4\pi\epsilon_0} \right)^2 \frac{4\pi z^2 N_0 Z \rho}{mc^2 \beta^2 A} \left[\ln\left(\frac{2mc^2 \beta^2}{I}\right) - \ln(1 - \beta^2) - \beta^2 \right] \quad (7.3)$$

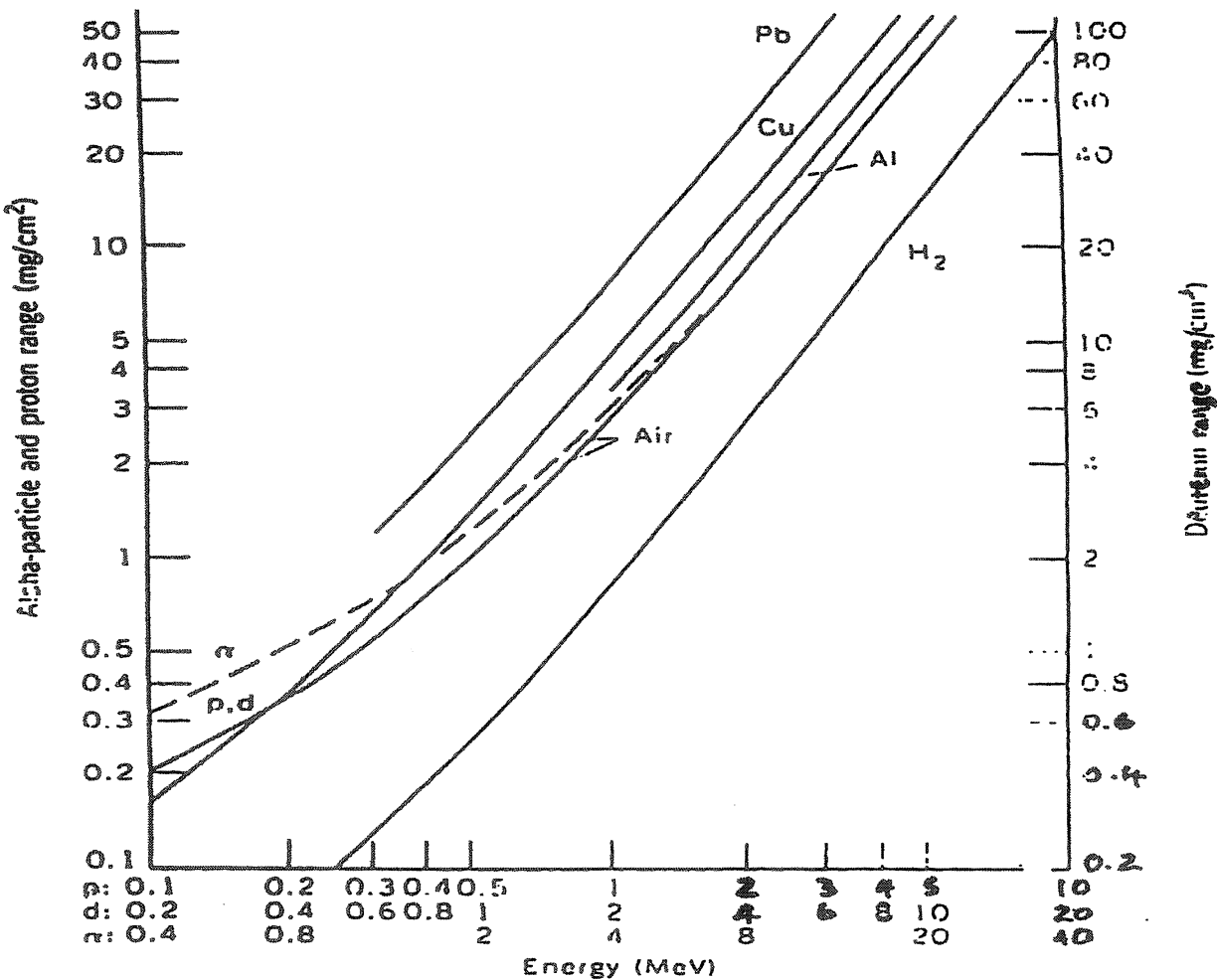


Figure 7.2 The range-energy relationship in various materials. Because the particles lose energy through scattering by atomic electrons, the range depends Inversely on the density. It is therefore convenient to plot the product range density. In units of mg/cm^2 . Unfortunately, this product is also called "range" in the literature. From A. H. Wapstra et al *Nuclear Spectroscopy Tables* (Amsterdam North-Holland, 1959).

where $v = \beta c$ is the velocity of the particle. ze is its electric charge. Z . A . and ρ are the atomic number, atomic weight, and density of the stopping material N is Avogadro's number and m is the electron mass. The parameter I represents the mean excitation energy of the atomic electrons, which

could in principle be computed by averaging over all atomic ionization and excitation processes In practice, I is regarded as an empirical constant, with a value in eV of the order of $10Z$.

In air, for instance, $I = 86 \text{ eV}$. while for Al, $I = 163 \text{ eV}$.

The range can he calculated by integrating Equation 7.3 over the energies of the particle.

$$R = \int_T^0 \left(-\frac{dE}{dx} \right)^{-1} dE \quad (7.4)$$

However, Equation 7.3 fails at low energy near the end of the range primarily.



Multifunction Digital Timer

Stock No. 343-997

Operating Instructions

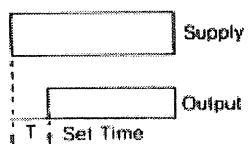
This timer is a multi time range, multi function digital timer fully programmable via two front panel push buttons, designed to fulfill the majority of time delay relay requirements. The timer may be operated from a wide range of supply voltages, 18 to 260V d.c. or a.c., without adjustment. An integral Ni-cad rechargeable battery ensures that the selected function and other stored settings will be retained in the event of a supply failure. In addition, with the battery in a suitably charged state it is possible to remotely programme the unit prior to installation.

A single pole changeover relay contact output is incorporated in the timer. An additional switch input, pin 11, is provided for the Delay on De-energise mode (DD) which can also be used as an enabling input in other modes. Where this facility is not required this input should be permanently connected to the supply, pin 2.

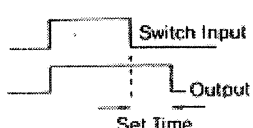
Operating Modes

Six operating modes are available, user selectable in the following sequence:

1. DE Delay on Energise - the output energises after the set time following the application of the supply.*



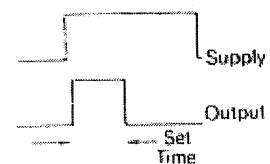
2. DD Delay on De-energise - this mode requires the supply to be maintained during the operation, control being effected by the switch input. The output relay energises immediately on closure of the switch (or by application of the supply if the switch is closed); when the switch input is opened the delay period is initiated and after the set time has elapsed, the output relay de-energises.



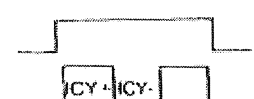
3. DP Delayed Pulse - output relay remains de-energised for the set time following application of the supply* and is then energised for 250msec only.



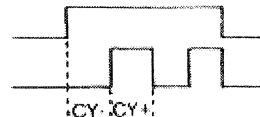
4. INT Interval - has the opposite action to DE in that the output energises immediately after the application of the supply* and de-energises after the set time has elapsed.



5. ICY Immediate cycle - the output relay energises after the application of the supply* for the ICY+ set time. The relay then de-energises for the ICY - set time and this cycle continues whilst the supply and switch input are maintained.



6. CY Cycle - the output relay remains de-energised for the CY - set time following the application of the supply*, then energises for the CY+ set time. This cycle continues whilst the supply and switch input are maintained.



* Alternatively the supply may be maintained and the switch input used to initiate the function.